

Extracellular Polymeric Substances (EPS) in a Hybrid Growth Membrane Bioreactor (HG-MBR): Viscoelastic and Adherence Characteristics

WANG YING,[†] FEI YANG,[†] AMOS BICK,[‡]
GIDEON ORON,[†] AND
MOSHE HERZBERG^{* ,†}

Zuckerberg Institute for Water Research, Ben Gurion University of the Negev, Sede Boqer Campus, Midreshet Ben Gurion, 84990, Israel, and Department of Industrial Engineering and Management, Jerusalem College of Technology, Jerusalem, Israel

Received July 9, 2010. Revised manuscript received September 24, 2010. Accepted September 29, 2010.

Extracellular polymeric substances (EPS) comprising the microbial biofilms in membrane bioreactor (MBR) systems are considered the most significant factor affecting sludge viscoelastic properties as well as membrane fouling. Understanding the water chemistry effects on EPS viscoelastic, conformational, and adherence properties are critical for defining the microbial biofilm's propensity of fouling the membrane surface. In this study, EPS extracted from a hybrid growth membrane bioreactor (HG-MBR) were analyzed for their adherence, viscoelastic properties and size distribution using quartz crystal microbalance with dissipation monitoring (QCM-D) and dynamic light scattering (DLS), respectively. Also, adsorption characteristics of EPS extracted from different locations in the HG-MBR (bioreactor liquor, fluidized carriers, and membrane surface) were defined and linked to the extent of the total polysaccharide content in the EPS. In accordance with the Derjaguin–Landau–Verwey–Overbeek (DLVO) theory, more EPS were adsorbed at higher ionic strength, lower pH and in the presence of calcium cations. Based on the QCM-D results, the calculated thickness of the EPS adsorbed layer was increased at lower ionic strength, higher pH, and only had a minor increase in the presence of calcium cations. The calculated shear modulus and shear viscosity suggest that at lower pH and in the presence of calcium, EPS becomes more viscous and elastic, respectively. DLS analysis correlated to the QCM-D results: A decrease in the hydrodynamic radius of the EPS colloids was observed at lower pH, and in the presence of calcium, most likely attributed to intermolecular attraction forces. Based on this study, low pH and presence of calcium may induce flocs' stability that resist erosion in the MBRs, while on the other hand, these conditions may induce the formation of an elastic and viscous EPS layer fouling the ultrafiltration (UF) membrane.

* Corresponding author phone: + 972 8 6563520; fax: + 972 8 6563503; e-mail: herzberg@bgu.ac.il.

[†] Ben Gurion University of the Negev.

[‡] Jerusalem College of Technology.

Introduction

A hybrid growth membrane bioreactor (HG-MBR) can be defined as the combination of a membrane separation process and a hybrid growth process, in which both suspended and attached-growth microorganisms are part of the membrane bioreactor (MBR) (1, 2). HG-MBR allows for upgrading the treatment capacities of existing MBR treatment plants by increasing biomass level. Since both attached- and suspended-growth are involved, the HG-MBR can be operated at lower mixed liquor suspended solids (MLSS) concentrations. Membrane fouling is minimized without loss of the treatment efficiency due to biological activity of the microorganisms that are attached to the supporting carries.

Membrane fouling can be described as a reduction in membrane performance, due to combined effects of several factors that cause clogging. Membrane clogging factors include biofouling, particles and colloids interception on the membrane surface, inorganic precipitates (scaling), and organics settling, all which can lead to an increase in hydraulic resistance over time and subsequently in reduced permeate flux (3). A number of factors affect membrane biofouling in MBRs, such as membrane characteristics, flow regime, operating conditions, and physicochemical properties of the mixed liquor and the sludge (3, 4).

Three fouling patterns can be identified in ultrafiltration (UF) membrane systems: (i) adsorption of either soluble microbial products (SMP) or extracellular polymeric substances (EPS) to the membrane surface; (ii) pore clogging by cell debris and colloids, and; (iii) sludge cake, or film formation arising from the deposition of cells or aggregates (3, 4). Adsorption of EPS is attributed to both physical and chemical adsorption that may change the friction factor in the membrane flow channels and cause a decrease in the flow area, which leads to a higher transmembrane pressure (TMP). Therefore, EPS can be removed by the shear stress of fluid mechanics, such as air scouring and liquid flow on the membrane surfaces. Chemical adsorption involves an elevated adhesion strength and energy between EPS and the membrane surfaces (Lewis acid/base force-induced adhesion), and is more resistant to shear stress. Consequently, cleaning agents must be used to remove chemically adsorbed EPS from the membrane surface (5).

EPS are metabolic products, resulting from active secretion from mainly sessile cells. EPS dominate the microenvironment of life of biofilm cells by filling and forming the space between the cells, shaping the three-dimensional biofilm structure. EPS characteristics determine the porosity, density, water content, charge, sorption properties, hydrophobicity, and mechanical stability of the biofilm microenvironment and can also be consumed as carbon and energy reserves during starvation (6, 7). EPS can be characterized by their relative levels of polysaccharides, proteins, nucleic acids, (phosphor-) lipids, and other polymeric compounds (8). In most cases, polysaccharides and proteins are the major constituents, whereas nucleic acids, uronic acids, (phosphor-) lipids, and humic substances are in smaller quantities (7, 9). The heterogeneous nature of the EPS mixture consists of both aromatic and aliphatic components with three main functional groups: carboxylic acids (COOH), phenolic alcohols (OH), and methoxy carbonyls (C=O) (10). EPS electric charge, derived mainly from the ionization of these groups, results in mutual repulsion and expansion of the biopolymers. Water chemistry affects EPS physicochemical characteristics, including conformation, charge, and hydrophilicity that in

turn have major impacts on EPS adherence properties and membrane fouling propensity (11, 12).

EPS adsorption and deposition on solid surfaces are affected by the interaction energies between the EPS constituents and a solid surface that can be predicted implementing Derjaguin–Landau–Verwey–Overbeek (DLVO) theory (13). This theory defines total interactions between a colloidal particle, in this case EPS and a substratum, as the sum of attractive van der Waals forces and repulsive electrostatic interactions (13, 14). The DLVO theory provides a good first approximation of the interacting force. Better approximation using the extended DLVO calculations (15, 16) (X-DLVO) takes into account thermodynamics that include other interaction forces, such as Lewis acid–base interactions, hydrophobic attraction and hydrophilic repulsion (17, 18). Applying the DLVO theory, it is widely known that solution chemistry plays a significant role in determining foulant–foulant and foulant–membrane physicochemical interactions, and hence membrane performance. Hong and Elimelech investigated the role of solution chemistry (ionic strength, divalent cations and pH) in natural organic matter (NOM) fouling of nanofiltration membranes using humic acid as a fouling model compound (19). Severe fouling was observed at higher electrolyte (NaCl) concentration, lower pH, and in presence of divalent cations (Ca^{2+}). Hence, these authors asserted that NOM adsorption and fouling follows the DLVO theory. Wang et al. found that Ca^{2+} and Mg^{2+} caused more severe fouling than once these cations are replaced with Na^+ (20). Divalent cations can chemically bridge between the membrane surface and the negatively charged humic acid molecules and also between the negatively charged carboxyl groups of the humic acid that were not in contact with the membrane (21).

EPS plays a major role in the cohesion of the sludge flocs and the biofilms matrix in the HG-MBR and its viscoelasticity can strongly affect the flocs and biofilm resistance to shear. Consequently, EPS viscoelasticity plays an important role in erosion of particles and colloids from the floc and biofilm surfaces in MBR systems and strongly related to the UF membrane fouling (22). Sludge properties, membrane filterability, and cleaning strategies are strongly influenced by EPS viscoelastic properties, which in turn are affected by feed solution chemistry (pH, ionic strength, and presence of divalent cations).

In this study, we were motivated to understand how the viscoelastic properties and adherence of EPS extracted from a laboratory scale HG-MBR are affected at different aquatic conditions. As previously studied by Kwon et al. (23), also here, but with real EPS, a quartz crystal microbalance with dissipation monitoring (QCM-D) was used for these analyses. QCM-D provides real-time, label free measurements of molecular adsorption and/or interactions taking place on various surfaces (24, 25). In addition to assessing adsorbed mass (ng/cm^2 sensitivity), measured as changes in oscillating frequency (F) of the quartz crystal, the energy dissipation (D), which is the reduced energy per oscillation cycle provides novel insights regarding structural properties of adsorbed layers (26, 27). Complementing the QCM-D analysis, the colloidal size distribution of EPS solutions was analyzed by dynamic light scattering (DLS) technique under all the aquatic conditions being studied. In addition, the composition and adherence properties of EPS originated from different locations in the HG-MBR were correlated.

Materials and Methods

HG-MBR Operation and Source of EPS. A hollow fiber UF membrane module of ZW-10 (Zenon Inc., Canada) with a nominal pore size of $0.04\ \mu\text{m}$ and a total filtering surface area of $0.93\ \text{m}^2$ was submerged in the center of a 190 L reactor. AqWise carriers (AqWise, Israel) made from high-density ($0.96\ \text{g}/\text{cm}^3$) polyethylene were filled as biofilm support. Detailed

information on the HG-MBR setup, operation, and process analysis is reported in our previous publication (28), in Supporting Information (SI) Figure S1 and in Table S1. Under constant-flux conditions, the increase in TMP and decrease in permeability were the indications for membrane fouling over time (SI Figure S2-A). This HG-MBR was used as a biomass source for EPS extraction and analysis of their adherence and viscoelastic properties. Sampling and analysis set up of the study is presented in Figure S3.

Biomass Concentration and EPS Extraction and Analysis. The attached biomass was determined by measuring the dry weights (at $105\ ^\circ\text{C}$) of 20 biofilm carriers before and after washing with 5% sodium hypochlorite and then calculated as biofilm concentration in the reactor and compared with the suspended biomass expressed as volatile MLSS (MLVSS). The MLVSS concentration was determined by measuring the volatile weight loss of the MLSS on ignition at $550\ ^\circ\text{C}$. Biomass concentrations in the HG-MBR are presented in SI Figure S2-B.

EPS extraction and analysis were performed from the MLSS, fluidized carriers, and a membrane fiber that was cutoff from the module (its ends were sealed) at the end of the run. EPS extraction was conducted by fixation step with 0.22% formaldehyde followed by addition of 1 N sodium hydroxide to facilitate dissociation of the acidic groups in the EPS to the solution (7). Thereafter, the suspension was centrifuged ($20\ 000\ \text{g}$, 15 min, $4\ ^\circ\text{C}$), filtered through a $0.22\ \mu\text{m}$ hydrophilic nylon filter (Millipore Co.), and dialyzed through a dialysis membrane of 3500 Da (Spectra/Por). Polysaccharide and protein contents in the EPS were analyzed colorimetrically according to Dubois et al. (29) and Bradford method (30), respectively.

QCM-D Analysis. EPS adherence and viscoelastic properties were analyzed during adsorption to silica coated crystals in a QCM-D under different pH values, ionic strength, and the presence of calcium. Two independent adsorption experiments were performed in the QCM-D under these aquatic conditions with similar results and one set of experimental data is presented in this study. The QCM-D measurements were performed with AT-cut quartz crystals mounted in an E1 system (Q-sense AB, Gothenburg, Sweden) (23). The crystals, with a fundamental resonant frequency of around 5 MHz, were coated with the amorphous silica by vapor deposition. Before each measurement, the crystals were soaked in a 5% ethylenediaminetetraacetic acid (EDTA) solution for 30 min, rinsed thoroughly with double distilled water, dried with pure N_2 gas, and treated for 10 min in a UV/O_3 (BioFORCE nanoscience) chamber.

Three sets of background solutions were prepared: (i) NaCl solutions with the ionic strength of 10 mM, 100 mM, and 1000 mM; (ii) NaCl solutions supplemented with 0.1 to 0.5 mM of CaCl_2 , adjusted to ionic strength of 10 mM; (iii) NaCl solutions (100 mM) with the pH values of 6.3 ± 0.1 , 7.3 ± 0.1 , and 8.3 ± 0.1 , adjusted with either NaOH or HCl. The EPS dissolved samples were prepared at concentration of 10.46 mg TOC/L with the corresponding background solution and filtered through a $0.22\ \mu\text{m}$ hydrophilic PVDF filter. All QCM-D experiments were performed under flow-through conditions using a digital peristaltic pump (IsmaTec, IDEX) operating in sucking mode. The pump tubing was connected to a glass vial containing the studied solutions that were injected to the sensor crystal chamber at $150\ \mu\text{L}/\text{min}$.

Prior to each of the QCM-D experiments and after cleaning the crystals, a baseline with double distilled water was acquired. For analyzing the effects of ionic strength and calcium cations on the EPS adsorption, thickness, and viscoelastic properties, solutions were injected sequentially to the QCM-D system in the following order: (i) background solution with the water chemistry studied; (ii) dissolved EPS in the background solution; (iii) similar background solution without EPS. Data

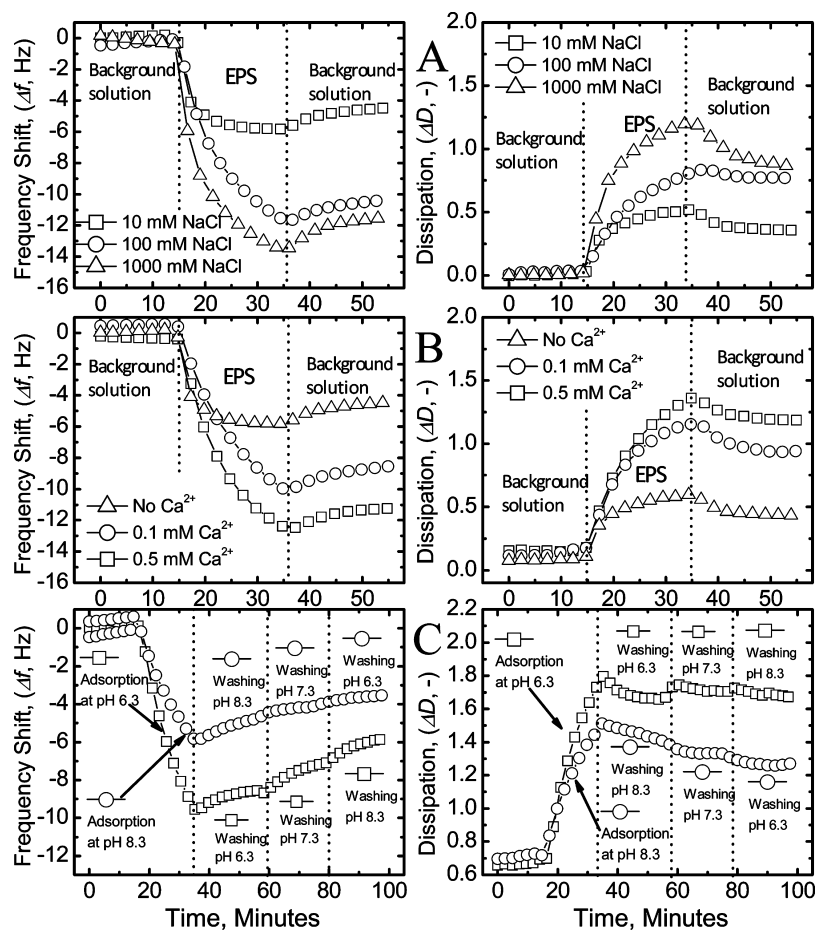


FIGURE 1. The effects of water chemistry parameters on the frequency and dissipation shifts during adsorption of EPS to silica coated quartz crystals: (A) Ionic strength; (B) Presence of calcium; and (C) pH of the background washing solution. EPS adsorbed layer was washed with background solution of the same water chemistry. An ambient pH of 6.2 ± 0.1 was measured during the analysis of the ionic strength and calcium effects. Calcium effect analysis was carried out in ionic strength of 10 mM adjusted with NaCl. The pH effect analysis was carried out in ionic strength of 100 mM NaCl solution.

is presented for the seventh overtone for comparison purposes of the aquatic conditions effects. For the effect of the ionic strength, changes in the frequency shift and dissipation were calculated by subtracting the decrease of the frequency caused by the background solution without EPS. In 1000, 100, and 10 mM NaCl, a decrease in the frequency of -19.5 , -2.3 , and -0.5 Hz at the seventh overtone were observed, respectively. The associated elevations of dissipation factors were 6.8, 0.8, and 0.1.

For analyzing the effect of pH on the EPS adsorption, thickness, and viscoelastic properties, solutions were injected sequentially to the QCM-D system in the following order: (i) 100 mM NaCl solutions adjusted to $\text{pH } 6.3 \pm 0.1$, or $\text{pH } 8.3 \pm 0.1$; (ii) the EPS dissolved studied solutions; (iii) this stage was applied for analyzing the reversibility and structural changes of the EPS adsorbed layer: After the EPS adsorption experiments at $\text{pH } 6.3 \pm 0.1$, solutions at elevated pH (6.3 ± 0.1 , 7.3 ± 0.1 , and 8.3 ± 0.1) without EPS were injected sequentially to the QCM-D flow cell. After the EPS adsorption experiments at $\text{pH } 8.3 \pm 0.1$, solutions at decreased pH (8.3 ± 0.1 , 7.3 ± 0.1 , and 6.3 ± 0.1) without EPS were injected sequentially to the QCM-D flow cell. For all experiments, frequency and dissipation shifts were collected for approximately 20 min for each stage.

Frequency variations (Δf , Hz) and dissipation factors (ΔD) were measured for three overtones ($n = 5, 7$, and 9). The viscoelastic properties of the EPS layers were calculated based on the Voigt model according to Voinova et al. (27). The density and viscosity of the solution used in this model were 1 g/cm^3 and $10^{-3} \text{ Pa}\cdot\text{s}$, respectively. The density of the

adsorbed layer was fixed at 1.030 g/cm^3 , following the recommendations of Gurdak et al. (31). The best fitting values of the shear viscosity (η), shear modulus (μ), and Voigt thickness (d_{Voigt}) of the adsorbed layer were obtained by modeling the experimental data of Δf and ΔD for three overtones using the program Q-Tools provided by Q-Sense AB (Sweden).

DLS Analysis. The distributions of diffusion coefficients for EPS were measured in all types of solutions applied in the QCM-D using dynamic light-scattering (CGS-3, ALV, Langen, Germany). Duplicates of lyophilized EPS samples were dissolved in the background solution being studied to a final concentration of 39.5 mg TOC/L. All samples were filtered in $0.22 \mu\text{m}$ hydrophilic PVDF filter (Millipore) prior to the measurement and 2.5 mL samples were placed in glass vials (Sigma-Aldrich, ISRAEL). The laser power was 20 mW at the He-Ne laser line (632.8 nm). Correlograms were calculated by ALV/LSE 5003 correlator, which were collected at 90° , during 10 s for 20 times, at 25°C . The correlograms were fitted with version of the program CONTIN (32) to calculate the decay time. Diffusion coefficients were calculated from the decay time distribution from which a weighted equivalent hydrodynamic radii were calculated by using the Stokes-Einstein equation.

Results and Discussion

EPS extracted from the suspended biofilm fraction of the HG-MBR, the MLSS, at solids retention time of 30 days, was used to form a stable adsorbed layer on a surface of a QCM-D

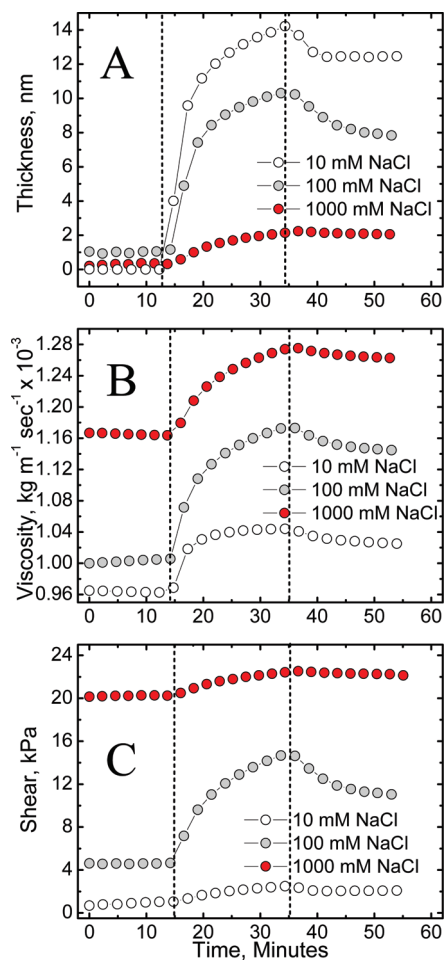


FIGURE 2. The effects of ionic strength on (A) the EPS layer thickness; (B) shear viscosity; and (C) shear modulus during adsorption experiment to silica coated quartz crystals. EPS adsorbed layer was washed with background solution of the same water chemistry. An ambient pH of 6.2 ± 0.1 was measured during the analysis of the ionic strength effects.

sensor for the viscoelasticity and conformation analysis at different aquatic conditions. In addition, changes in the hydrodynamic radius for the dissolved mixture of the EPS molecules were analyzed using DLS and compared the QCM-D results. Under these conditions, total proteins and polysaccharides concentrations in the EPS were 15.8 ± 2.11 and 8.1 ± 1.12 mg/L, respectively. Figure 1 shows the frequency and dissipation shifts under all conditions during adsorption and washing stages of the EPS layer formed on the QCM-D sensors. The effects of the following parameters on the adsorbed and dissolved EPS conformation were analyzed by the QCM-D and DLS, respectively: (i) ionic strength, (ii) calcium cations, and (iii) pH.

The Effect of Ionic Strength on EPS Adsorption and Viscoelastic Properties. The effect of ionic strength on EPS adsorption, viscoelastic properties, and hydrodynamic radius are illustrated in Figures 1, 2, and 5, respectively. It is likely that at high ionic strength, the charges of the silica surface and EPS macromolecules are significantly shielded, due to electric double layer compression and charge screening, leading to a decrease in electrostatic repulsion between the silica surface and adsorbed EPS film. Consequently, EPS enhanced deposition rate is represented by the higher frequency and dissipation shifts of the silica coated crystal (Figure 1 A). The calculated thicknesses of the adsorbed EPS layers were 3, 10, and 14.5 nm in 1000 mM, 100 mM, and 10 mM NaCl background solution, respectively (Figure 2 A), using the Voigt-based model (27). Due to reduced interchain

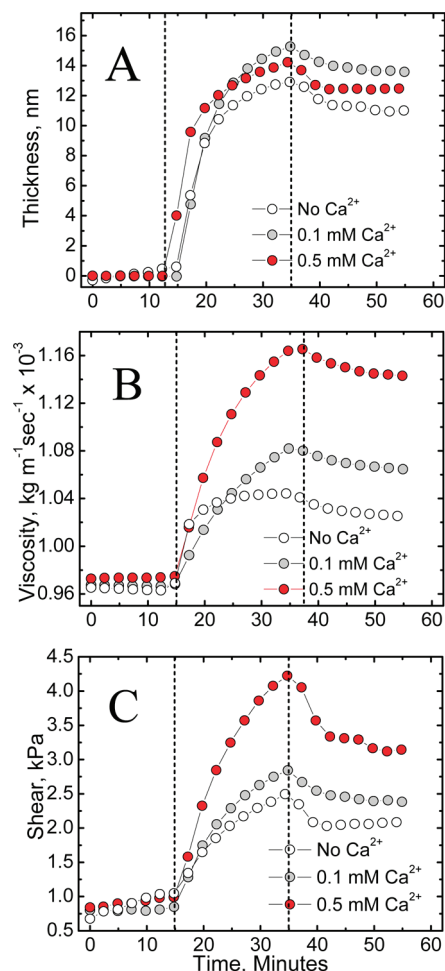


FIGURE 3. The effects of the presence of calcium on (A) the EPS layer thickness; (B) shear viscosity; and (C) shear modulus during adsorption experiment to silica coated quartz crystals. EPS adsorbed layer was washed with background solution of the same water chemistry. An ambient pH of 6.2 ± 0.1 was measured during the analysis of the calcium effects. The calcium effect analysis was carried out in ionic strength of 10 mM adjusted with NaCl.

electrostatic repulsion at high ionic strength, EPS macromolecules become coiled and spherical in shape (10), forming a more compact layer. Thus, the thickness of the adsorbed layer at 1000 mM was the lowest. At low ionic strength, on the other hand, strong electrostatic repulsion between the silica surface and EPS hinders EPS deposition. Thus, lower frequency and dissipation shifts were observed. At lower ionic strength, the long-range of the electric double layer repulsion prevents the formation of closely packed EPS adsorbed layer, which has a higher observed thickness (Figure 2 A). It should be mentioned that changes in the conformation of the EPS layer are likely to change the layer compactness. Using the Voigt model, we compared the viscoelastic properties of the EPS assuming layer density with constant value of 1.03 g/cm^3 . The use of constant layer density of 1.03 g/cm^3 was justified by a study of Gurdak et al. (31) who showed that when using the Voigt model, an uncertainty of the layer density within a range of pure water and pure protein layer ($1\text{--}1.4 \text{ g/cm}^3$) had negligible effects on the best computed fitted thickness, shear viscosity, and shear modulus values.

Corroborating with the QCM-D results, comparable changes in the hydrodynamic radius of the EPS molecules were analyzed with DLS. At ionic strength of 10, 100, and 1000 mM, the major distribution of the EPS colloids were at 3, 1.3, and 0.7 nm of calculated equivalent hydrodynamic

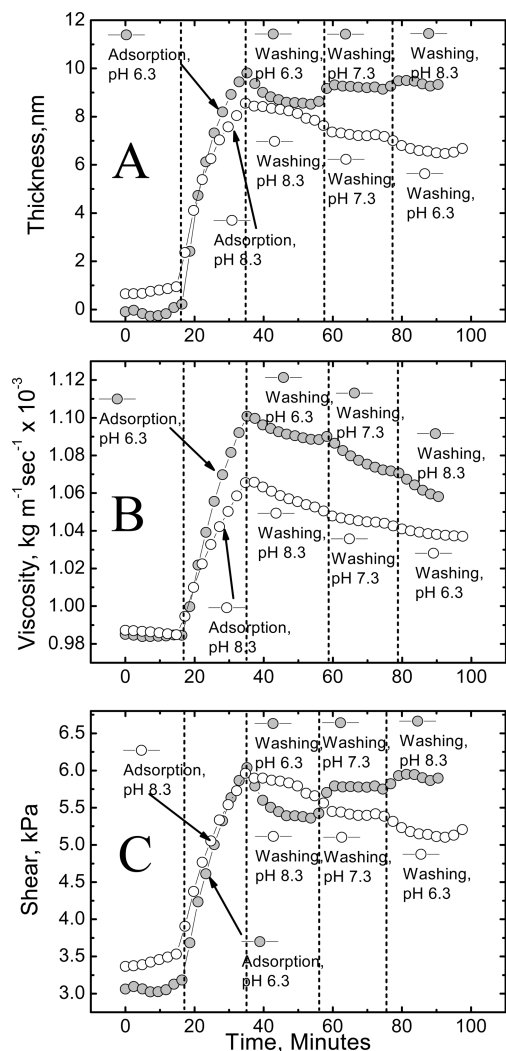


FIGURE 4. The effect of pH on the (A) EPS layer thickness; (B) viscosity; (C) and shear modulus during adsorption experiment to silica coated quartz crystals. EPS adsorbed layer was washed with similar background solution (100 mM NaCl) at different pH values.

radii, respectively (Figure 5A). For the ionic strength of 100 mM, an additional small group of EPS colloids are distributed with a peak value at 3.5 nm. This additional small group of colloids is probably attributed to small EPS aggregates.

The effects of ionic strength on intrinsic changes of the water interface viscosity and shear modulus are observed at the first stage of the experiment when background solution was injected to the QCM-D flow cell (Figure 2B, C). If we only take into account the contribution of the EPS layer to the increase of the shear modulus and viscosity values, the highest elevation in both parameters was observed for 100 mM NaCl comparing to background solutions of 1000 mM and 10 mM NaCl (Figure 2 C). We do not have an explanation to this viscoelastic behavior.

The Effect of Calcium Cations on EPS Adsorption and Viscoelastic Properties. The effect of calcium cations (Ca^{2+}) on EPS adsorption, viscoelastic properties, and hydrodynamic radius are illustrated in Figures 1, 3, and 5, respectively. In these experiments, the highest frequency and dissipation shifts were observed at the highest Ca^{2+} concentration (Figure 1 B) clearly demonstrating how calcium is dramatically increasing EPS adsorption. Unlike Na^+ , Ca^{2+} binds specifically through complex formation with the acidic functional groups (predominantly carboxylic) of the EPS (33). Thus, in the presence of calcium ions, the charge of the EPS is reduced

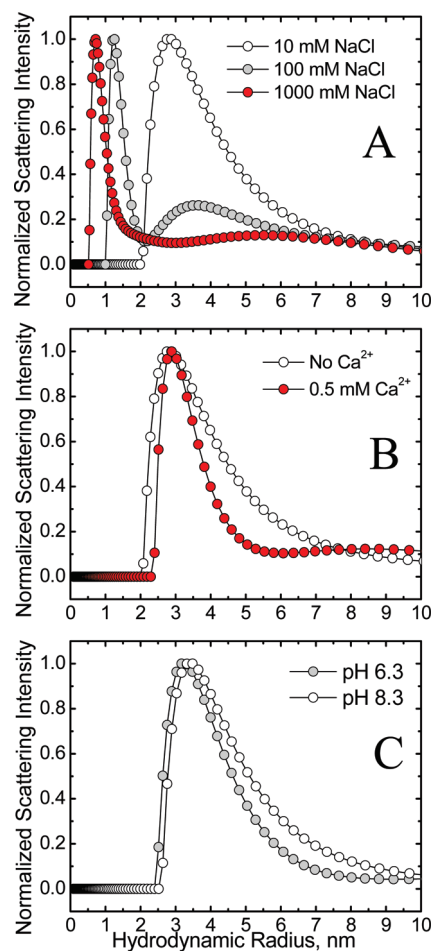


FIGURE 5. The effects of ionic strength (A), presence of calcium (B), and pH (C) on the distribution of the hydrodynamic radius of the EPS colloids measured in a DLS. EPS concentration was 39.5 mg TOC/L. The effect of calcium cations was analyzed under ionic strength of 10 mM adjusted with NaCl. The pH effect analysis was carried out in ionic strength of 100 mM NaCl solution.

significantly not only due to effective charge screening but also due to complex formation. The substantial decrease in EPS charge in the presence of calcium ions, as well as the silica surface, results in an increased deposition rate of EPS (Figure 1B). Reduced interchain electrostatic repulsion of EPS due to calcium complexation also results in the formation of small and coiled macromolecules. Subsequently, a more compact EPS fouling layer is formed. As observed by the DLS technique, particle size distribution is narrower in the presence of 0.5 mM calcium cations (Figure 5B). Figures 3B and C show an increase in the layer shear viscosity and shear modulus meaning the layer is becoming more viscous and elastic in the presence of calcium. The adsorbed EPS layer became more elastic by the presence calcium cations in a dose response manner: the calculated shear modulus values were 4.25×10^3 Pa, 3×10^3 Pa, and 2.8×10^3 Pa for calcium cation concentrations of 0.5 mM, 0.1 mM, and 0 mM, respectively (Figure 3 C). Also, an increased viscosity of the EPS layer was observed and the calculated viscosities were 0.00103 $\text{kg/m}\cdot\text{s}$, 0.00108 $\text{kg/m}\cdot\text{s}$, and 0.0016 $\text{kg/m}\cdot\text{s}$, for calcium cation concentrations of 0.0 mM, 0.1 mM, and 0.5 mM, respectively (Figure 3 B). These differences between the viscoelastic properties may indicate that the conformation of the adsorbed EPS layer changed at different Ca^{2+} concentrations. In contrast to the changes observed for the viscoelastic properties of the EPS, Figure 3 A shows that calcium cations had only minor effects on the thickness of

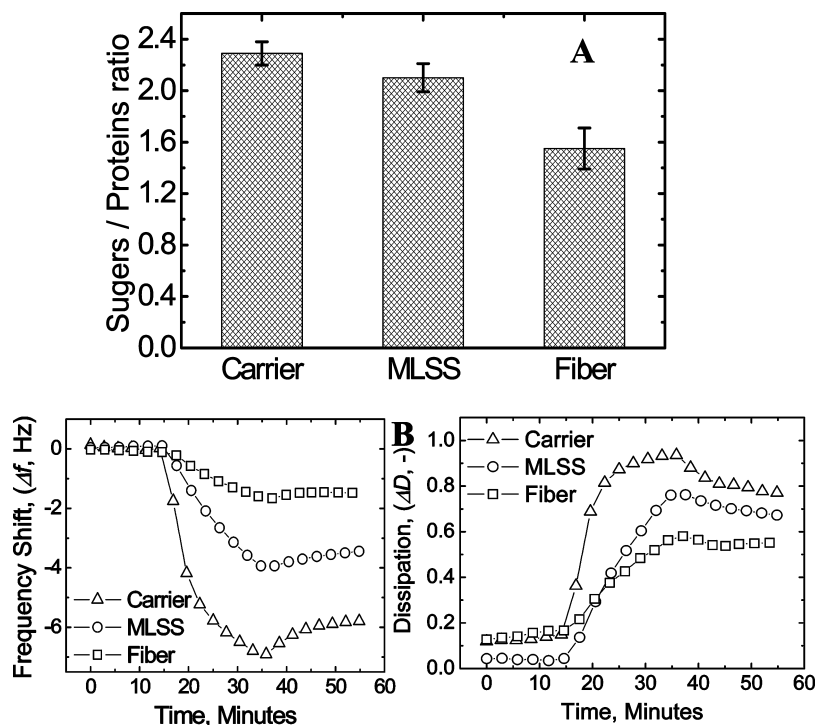


FIGURE 6. The effect of polysaccharides (PS)/proteins (PN) ratio on EPS adsorption kinetic in a QCM-D: (A) PS/PN ratio in EPS extracted from different locations in the HG-MBR system—MLSS, attached growth on the carrier, and membrane surface fouling layer; (B) Frequency and dissipation shifts during adsorption of the associated EPS presented in (A).

the adsorbed EPS layer. Conformational changes of the EPS induced by calcium are observed by the DLS analysis, in which a narrower size distribution of the EPS colloids is observed. Hence, presence of calcium is likely to induce strong bridging within the biopolymers. These results can explain both the higher adsorption of EPS in the presence of calcium where more compacted molecules with higher diffusion coefficient are introduced to the QCM-D flow cell (as analyzed by the DLS, the particle size distribution due to the presence of calcium was mainly reduced for the larger particles that had higher scattering intensity). When an EPS layer is formed on the QCM-D sensor, the calcium may form dimers between polysaccharides in the EPS that are well compacted such as suggested for polygalacturonic acid (PGA) by others (34).

The Effect of pH on EPS Adsorption and Viscoelastic Properties. The influence of pH on EPS adsorption, viscoelastic properties, and hydrodynamic radius is shown in Figures 1, 4, and 5, respectively. At lower pH, increased amount of protonated carboxylic and hydroxylic functional groups reduce the negative charge, the acidity, and the hydrophilic nature of the EPS. In order to make sure that indeed EPS is deprotonated at the pH range tested here, 10 mL of similar EPS solution used in the QCM-D analysis (10.46 mg TOC/L) in DI water was titrated with 1 mM NaOH solution after acidifying the EPS solution with HCl (SI Figure S3). Major pH changes were observed between pH values of 4.5 and 9. Hence, our range (pH 6.3 to pH 8.3) of pH effect was right in the middle of the range where EPS protonation–deprotonation process occurs. Surface charge of the silica surface becomes less negative with the decrease of the pH and is neutralized at pH 3, which is the isoelectric point of the silica (35). Hence, higher EPS adsorption is observed at the lower pH of 6.3 compared to pH 8.3 (Figure 1 C). It is most likely due to the charge reduction of the silica surface as well as of the EPS macromolecules, in which more carboxylic and hydroxylic groups of EPS become protonated with reduced pH. Consequently, the electrostatic repulsion between the silica surface and EPS, and between EPS contained in solution

and the deposited EPS is reduced at pH 6.3. Moreover, EPS has a smaller macromolecular configuration at pH 6.3, due to reduced electrostatic repulsion between neighboring functional groups, and thus forms a denser adsorbed layer. DLS analysis (Figure 5 C) confirmed this hypothesis in which larger colloids in the EPS solution are detected at pH 8.3. The effects of the pH were further analyzed during washing of the adsorbed EPS layer with a similar background solution, without EPS, at different pH values. After adsorption of the EPS to the crystal at pH 6.3, an increase in the EPS thickness was observed once the layer was washed with the background solution at elevated pH (Figure 4A). In similar manner, however, opposite trend, once the layer was washed with the background solution at decelerated pH values, a decrease in the EPS thickness was observed (Figure 4A). The pH also had a significant effect on the elasticity of the EPS adsorbed layer: A lower shear modulus of the EPS layer was observed when the background solution at decreasing pH values was used to wash the EPS layer in a dose response manner (Figure 4 C). In a similar however, opposite trend, a higher shear modulus of the EPS layer was observed when the background solution at elevated pH values was used to wash the EPS layer (Figure 4C). These results imply that at elevated pH, induced hydration of the EPS layer increases EPS thickness and elasticity (Figure 4C). A decrease of the EPS viscosity was observed for both washes at pH values of 6.3 and 8.3 but at different rates (Figure 4B). Washing the EPS layer at elevated pH values showed an increasing rate of decline in viscosity while at decelerated pH values the decline in viscosity was stabilized at pH 6.3. Possible explanation for these results is hydration of the EPS layer with coupled water at different rates according to the pH of the washing solution. At higher pH, EPS consist of more deprotonated functional groups (mainly carboxylic) and hydration process is likely to be faster than at lower pH when more functional groups are protonated and the EPS structure is more coiled. Hence, DLS analysis shows a slightly smaller size distribution at lower pH of 6.3 (Figure 6C).

Analyzing Adherence of EPS Extracted from Different Locations in the HG-MBR. Recent studies revealed a strong relationship between EPS cohesion and polysaccharide concentration (12). At the end of the fouling experiment in the HG-MBR, EPS was extracted from the MLSS, the carriers' surface, and the membrane surface. Since the ratio of the polysaccharides to proteins (PS/PN) in the extracted EPS samples from the reactor was different, we tried to relate PS/PN ratio to the adherence kinetics of the EPS extracted from three different locations in the HG-MBR using the QCM-D. Figure 6 describes a close relationship between the PS/PN ratios in the EPS extracted from the different locations in the reactor to the adherence properties of EPS that may consequently affect the membrane performance. Figure 6B, C describes the decrease in frequency and increase in dissipation energy of the quartz crystal due to EPS adsorption to the silica surface. Interestingly, consistent with the PS/PN values, the highest and lowest adsorption rates were observed for the EPS extracted from the carriers and the membrane fiber, respectively. While this relationship corroborates with other studies, where polysaccharides content in EPS induce adherence properties, it is not clear why there are changes in the type and specially adherence properties, of EPS distributed in the HG-MBR. The extracted EPS from the fiber surface was less adhesive than the EPS extracted from the carriers. A possible explanation for this difference is the penetration of EPS into the UF membrane pores that are protected from shear forces while the impact of the fluid shear forces on the carriers and the MLSS aggregates is higher. The higher shear on the carriers and the MLSS allows better selection of more adhesive constituents in the EPS matrix to remain and eventually the EPS is left with higher fraction of polysaccharides. The major role of proteins in the UF MBR fouling was already shown by Metzger et al (2007). Irreversible organic fouling of the UF membrane in MBR was found to be predominated by bound proteins originated from SMP of the MBR biomass (36).

Implications of EPS Adherence and Viscoelastic Characterization Using QCM-D. In this study, we delineated water chemistry effects on EPS viscoelastic properties. As well, the effects on conformation and adherence characteristics to silica surface were examined. Even though the EPS extracted from a domestic wastewater had heterogeneous nature in its composition, the viscoelastic properties, conformation, and adherence characteristics corroborate with other fundamental fouling studies that used various model fouling agents (20, 21, 25). Since the QCM-D adsorption experiments carried out in this study, were conducted on a silica surface, only general conclusions regarding EPS adherence to a UF membrane surface can be drawn. EPS is the major sludge floc component keeping it in a three-dimensional matrix. Therefore, understanding the EPS viscoelasticity and cohesion characteristics is critical. It was shown that EPS viscoelasticity and cohesion properties are influenced by ionic strength, pH, and presence of calcium cations. Using the QCM-D technique, it was shown that EPS becomes more viscous and elastic in the presence of calcium and at low pH, more viscous. These conditions, on one hand, are most likely favorable for inducing stable flocs in the HG-MBR, however, may induce the formation of an elastic and viscous fouling EPS layer on the UF membrane. Using DLS analysis of the EPS solution, it was shown that in the presence of calcium, at low pH, and at high ionic strength, reduction in the intermolecular repulsive interactions contracts the colloidal size distribution. These results corroborate with the higher adsorption rates at similar conditions in the QCM-D flow cell attributed also to the higher diffusion coefficients for smaller EPS colloids. Also the formation of more viscous and elastic layer, in the presence of calcium, can be explained by the DLS results where a decrease in intermolecular repulsive

interactions is presumed. It was also shown that different locations in the HG-MBR provide different niches for biofilm formation that produce EPS with diverse adherence properties and polysaccharide content. QCM-D allows fast characterization of EPS adherence, adsorption/desorption, and viscoelasticity under various aquatic conditions, flow regimes, and surfaces that mimic membranes used for water treatment. Furthermore, defining best conditions for desorption of EPS can be carried out rapidly, using different cleaning agents for its removal from the surface. Isolating the EPS components, their contribution to the overall adherence and compactness may be defined and highly efficient biofouling control strategies can be adopted.

Acknowledgments

We gratefully acknowledge the support received from the joint BMBF-MOST German-Israeli Research Program, Project No. WT0902.

Supporting Information Available

Table S1 and Figures S1-S4. This material is available free of charge via the Internet at <http://pubs.acs.org>.

Literature Cited

- Yang, Q. Y.; Chen, J. H.; Zhang, F. Membrane fouling control in a submerged membrane bioreactor with porous, flexible suspended carriers. *Desalination* **2006**, *189*, 292-302.
- Sombatsompop, K.; Visvanathan, C.; Ben Aim, R. Evaluation of biofouling phenomenon in suspended and attached growth membrane bioreactor systems. *Desalination* **2006**, *201*, 138-149.
- Le-Clech, P.; Chen, V.; Fane, T. A. G. Fouling in membrane bioreactors used in wastewater treatment. *J. Membr. Sci.* **2006**, *284*, 17-53.
- Liao, B. Q.; Bagley, D. M.; Kraemer, H. E.; Leppard, G. G.; Liss, S. N. A review of biofouling and its control in membrane separation bioreactors. *Water Environ. Res.* **2004**, *76*, 425-436.
- Flemming, H. C.; Griebe, T.; Schaule, G. Antifouling strategies in technical systems—A short review. *Water Sci. Technol.* **1996**, *34*, 517-524.
- Flemming, H. C.; Neu, T. R.; Wozniak, D. J. The EPS matrix: The "House of Biofilm cells. *J. Bacteriol.* **2007**, *189*, 7945-7947.
- Liu, H.; Fang, H. H. P. Extraction of extracellular polymeric substances (EPS) of sludges. *J. Biotechnol.* **2002**, *95*, 249-256.
- Laspidou, C. S.; Rittmann, B. E. A unified theory for extracellular polymeric substances, soluble microbial products, and active and inert biomass. *Water Res.* **2002**, *36*, 2711-2720.
- Comte, S.; Guibaud, G.; Baudu, M. Relations between extraction protocols for activated sludge extracellular polymeric substances (EPS) and complexation properties of Pb and Cd with EPS Part II. Consequences of EPS extraction methods on Pb²⁺ and Cd²⁺ complexation. *Enzyme Microb. Technol.* **2006**, *38*, 246-252.
- Tsuneda, S.; Aikawa, H.; Hayashi, H.; Yuasa, A.; Hirata, A. Extracellular polymeric substances responsible for bacterial adhesion onto solid surface. *FEMS Microbiol. Lett.* **2003**, *223*, 287-292.
- Frank, B. P.; Belfort, G. Intermolecular forces between extracellular polysaccharides measured using the atomic force microscope. *Langmuir* **1997**, *13*, 6234-6240.
- Frank, B. P.; Belfort, G. Polysaccharides and sticky membrane surfaces: critical ionic effects. *J. Membr. Sci.* **2003**, *212*, 205-212.
- Derjaguin, B. V. A theory of the heterocoagulation, interaction and adhesion of dissimilar particles in solutions of electrolytes. *Discuss. Faraday Soc.* **1954**, *18*, 85-98.
- Poortinga, A. T.; Bos, R.; Busscher, H. J. Reversibility of bacterial adhesion at an electrode surface. *Langmuir* **2001**, *17*, 2851-2856.
- Azeredo, J.; Visser, J.; Oliveira, R. Exopolymers in bacterial adhesion: Interpretation in terms of DLVO and XDLVO theories. *Colloids Surf., B* **1999**, *14*, 141-148.
- Dentini, M.; Coviello, T.; Burchard, W.; Crescenzi, V. Solution properties of exocellular microbial polysaccharides. 3. Light scattering from gellan and from the exocellular polysaccharide of *Rhizobium trifolii* (strain TA-1) in the ordered state. *Macromolecules* **1988**, *21*, 3312-3320.

- (17) Bos, R.; van der Mei, H. C.; Busscher, H. J. Physico-chemistry of initial microbial adhesive interactions - its mechanisms and methods for study. *FEMS Microbiol. Rev.* **1999**, *23*, 179–230.
- (18) Jucker, B. A.; Zehnder, A. J. B.; Harms, H. Quantification of polymer interactions in bacterial adhesion. *Environ. Sci. Technol.* **1998**, *32*, 2909–2915.
- (19) Hong, S. K.; Elimelech, M. Chemical and physical aspects of natural organic matter (NOM) fouling of nanofiltration membranes. *J. Membr. Sci.* **1997**, *132*, 159–181.
- (20) Wang, Z.; Zhao, Y. Y.; Wang, J. X.; Wang, S. C. Studies on nanofiltration membrane fouling in the treatment of water solutions containing humic acids. *Desalination* **2005**, *178*, 171–178.
- (21) Jucker, C.; Clark, M. M. Adsorption of aquatic humic substances on hydrophobic ultrafiltration membranes. *J. Membr. Sci.* **1994**, *97*, 37–52.
- (22) Mikkelsen, L. H. The shear sensitivity of activated sludge - Relations to filterability, rheology and surface chemistry. *Colloid Surf., A* **2001**, *182*, 1–14.
- (23) Kwon, K. D.; Green, H.; Bjoorn, P.; Kubicki, J. D. Model bacterial extracellular polysaccharide adsorption onto silica and alumina: Quartz crystal microbalance with dissipation monitoring of dextran adsorption. *Environ. Sci. Technol.* **2006**, *40*, 7739–7744.
- (24) Eydelnant, I. A.; Tufenkji, N. Cranberry derived proanthocyanidins reduce bacterial adhesion to selected biomaterials. *Langmuir* **2008**, *24*, 10273–10281.
- (25) Wang, X.; Ruengruglikit, C.; Wang, Y. W.; Huang, Q. Interfacial interactions of pectin with bovine serum albumin studied by quartz crystal microbalance with dissipation monitoring: Effect of ionic strength. *J. Agric. Food Chem.* **2007**, *55*, 10425–10431.
- (26) Nguyen, T. H.; Elimelech, M. Adsorption of plasmid DNA to a natural organic matter-coated silica surface: Kinetics, conformation, and reversibility. *Langmuir* **2007**, *23*, 3273–3279.
- (27) Voinova, M. V.; Rodahl, M.; Jonson, M.; Kasemo, B. Viscoelastic acoustic response of layered polymer films at fluid-solid interfaces: Continuum mechanics approach. *Phys. Scr.* **1999**, *59*, 391–396.
- (28) Ying, W.; Herzberg, M.; Yang, F.; Bick, A.; Oron, G. Hybrid growth membrane bioreactor (HG-MBR): The indirect impact of sludge retention time on membrane fouling. *Desalin. Water Treat.* **2009**, *10*, 27–32.
- (29) Dubois, M.; Gilles, K. A.; Hamilton, J. K.; Rebers, P. A.; Smith, F. Colorimetric method for determination of sugars and related substances. *Anal. Chem.* **1956**, *28*, 350–356.
- (30) Bradford, M. A rapid and sensitive method for the quantitation of microgram quantities of protein utilizing the principle of protein dye-binding. *Anal. Biochem.* **1977**, *72*, 248–254.
- (31) Gurdak, E.; Dupont-Gillain, C. C.; Booth, J.; Roberts, C. J.; Rouxhet, P. G. Resolution of the vertical and horizontal heterogeneity of adsorbed collagen layers by combination of QCM-D and AFM. *Langmuir* **2005**, *21*, 10684–10692.
- (32) Provencher, S. W. CONTIN: A general purpose constrained regularization program for inverting noisy linear algebraic and integral equations. *Comput. Phys. Commun.* **1982**, *27*, 229–242.
- (33) Hering, J. G.; Morel, E. M. *Principles and Applications of Aquatic Chemistry*; Wiley, John & Sons: New York, 1992.
- (34) de Kerchove, A. J.; Elimelech, M. Formation of polysaccharide gel layers in the presence of Ca²⁺ and K⁺ ions: Measurements and mechanisms. *Biomacromolecules* **2006**, *8*, 113–121.
- (35) Nguyen, T. H.; Chen, K. L. Role of divalent cations in plasmid DNA adsorption to natural organic matter-coated silica surface. *Environ. Sci. Technol.* **2007**, *41*, 5370–5375.
- (36) Metzger, U.; Le-Clech, P.; Stuetz, R. M.; Frimmel, F. H.; Chen, V. Characterisation of polymeric fouling in membrane bioreactors and the effect of different filtration modes. *J. Membr. Sci.* **2007**, *301*, 180–189.

ES102309Y